This article was downloaded by: *10.2.97.136*
On: 30 May 2023
Access details: *subscription number*
Publisher: *CRC Press*
Informa Ltd Registered in England and Wales Registered Number: 1072954 Registered office: 5 Howick Place, London SW1P 1WG, UK

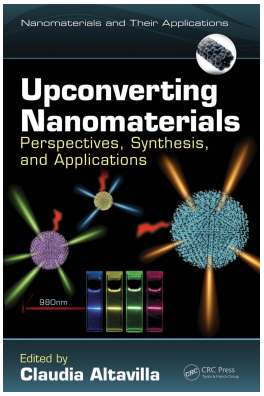


# Upconverting Nanomaterials Perspectives, Synthesis, and Applications

Claudia Altavilla

## Principle of Luminescence Upconversion and Its Enhancement in Nanosystems

Publication details
https://test.routledgehandbooks.com/doi/10.1201/9781315371535-4
Hong Zhang, Langping P. Tu, Xiao Min Liu
**Published online on: 10 Oct 2016**

**How to cite :-** Hong Zhang, Langping P. Tu, Xiao Min Liu. 10 Oct 2016, *Principle of Luminescence Upconversion and Its Enhancement in Nanosystems from:* Upconverting Nanomaterials, Perspectives, Synthesis, and Applications CRC Press
Accessed on: 30 May 2023
https://test.routledgehandbooks.com/doi/10.1201/9781315371535-4

**PLEASE SCROLL DOWN FOR DOCUMENT**

Full terms and conditions of use: https://test.routledgehandbooks.com/legal-notices/terms

This Document PDF may be used for research, teaching and private study purposes. Any substantial or systematic reproductions, re-distribution, re-selling, loan or sub-licensing, systematic supply or distribution in any form to anyone is expressly forbidden.

The publisher does not give any warranty express or implied or make any representation that the contents will be complete or accurate or up to date. The publisher shall not be liable for an loss, actions, claims, proceedings, demand or costs or damages whatsoever or howsoever caused arising directly or indirectly in connection with or arising out of the use of this material.

Downloaded By: 10.2.97.136 At: 04:36 30 May 2023; For: 9781315371535, chapter2, 10.1201/9781315371535

# 2

# *Principle of Luminescence Upconversion and Its Enhancement in Nanosystems*

**Hong Zhang, Langping P. Tu, and Xiao Min Liu**

**CONTENTS**



## 2.1 Principle of Upconversion Luminescence in Nanosystems

Most emissions are down conversion (DC) in nature, which means that the emission energy is lower than the excitation energy. In this book, we introduce an opposite concept—upconversion (UC) emission—the emission of one higher energy photon upon the excitation of several lower energy photons. The latter is very attractive for applications in data storage, multicolor displays, photovoltaic devices, biological field, etc. In recent years, the development of nanotechnology has been increasingly inviting scientific interest, especially the interest of the biomedical field, in relevant material systems such as lanthanide (Ln) ions doped materials. In these materials, near-infrared (NIR) photons are converted to higher energy photons ranging from ultraviolet (UV) to NIR. Here, the excitation wavelengths are especially

Downloaded By: 10.2.97.136 At: 04:36 30 May 2023; For: 9781315371535, chapter2, 10.1201/9781315371535

seductive to the biomedical field since it falls in the so-called "optical window" (~650–1300 nm), that is, the spectral range of minimal absorption of human tissue. Besides, auto-fluorescence of the biological background is negligible under the NIR excitation. All these unique features make these materials, once in nanometer sizes, ideal candidates for contrast agents of luminescence imaging. Their application potential is also expanded to solar energy utilization by converting the NIR part of the solar spectrum into visible range in order to match the absorption of commercially available solar cells.

The UC luminescence originates from the peculiar electronic property of lanthanide ions. The lanthanides are a group of elements in the periodic table where the 4f inner shell is filled with electrons. They are mostly stable in trivalent form and the $Ln^{3+}$ ions have the electronic configuration $4f^n5s^25p^6$ where $n$ varies from 0 to 14. The shielding of the 4f electrons of $Ln^{3+}$ by the completed filled $5s^2$ and $5p^6$ subshells results in weak electron–phonon coupling which is responsible for important phenomena such as sharp and narrow f – f transition bands. In addition, the f – f transitions are in principle parity forbidden, but the forbidden can be partially released when the ions locate in a crystals field, where the mixture of states of different parities results in low transition probabilities and substantially long-lived excited states. Moreover, most of the lanthanides have a great many energy levels, some of them are arranged ladder-like, which facilitates UC process according to the successive photon absorption or energy transfer. Consequently, UC emission is theoretically expected for most of lanthanide ions (e.g., $Er^{3+}$, $Tm^{3+}$, and $Ho^{3+}$). The UC emission of these materials is usually termed "upconversion luminescence."

The physics of the UC luminescence has been explored since the 1960s. Thanks to the pioneering work reported by Auzel and others in theoretical and experimental studies, several mechanisms of UC have been proposed (Auzel 2004), including excited-state absorption (ESA), energy transfer upconversion (ETU), photon avalanche (PA), and cooperative sensitization upconversion (CSU). More recently, with the help of specially designed nanostructures, an energy migration-mediated upconversion (EMU) mechanism was proposed (F. Wang et al. 2011). Now, let us review them one by one.

### 2.1.1 Traditional UC Mechanisms

ESA is the simplest UC mechanism. As seen in Figure 2.1, in this mechanism, sequential absorption within the levels of a given $Ln^{3+}$ ion is responsible for UC emission. Owing to the well ladder-like energy levels of some lanthanide activator ions and the long lifetimes of the intermediate excited energy levels (range from tens of microseconds to milliseconds), the ESA process could theoretically take place in many of the singly doped lanthanide activator ions (e.g., $Er^{3+}$, $Tm^{3+}$, $Ho^{3+}$, $Pr^{3+}$, and $Dy^{3+}$). It should be noted that ESA only plays an important role when the doping concentration is relatively low, that

Downloaded By: 10.2.97.136 At: 04:36 30 May 2023; For: 9781315371535, chapter2, 10.1201/9781315371535

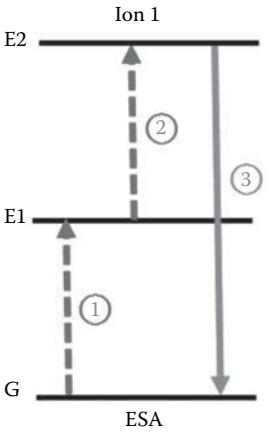


**FIGURE 2.1**
Schematic diagram of ESA process.

is, energy transfer between two activators is negligible, which leads to insufficient absorption and low UC efficiency.

In the case of ETU, UC emission is induced by the energy transfer between two $Ln^{3+}$ ions, named as activator and sensitizer, respectively. As seen in Figure 2.2a, when both of them are in excited states, UC is assumed to take place to lift the activator onto a higher excited state at the expense of the excitation energy of the sensitizer. The energy transfer probability $P_{SA}$ can generally be written as

$$P_{SA} = \frac{(R_0/R)^S}{\tau_S} \tag{2.1}$$

where $\tau_S$ is the actual excited state lifetime of the sensitizer, $R_0$ is the critical energy transfer distance for which excitation energy transfer and spontaneous deactivation of the sensitizer have equal probabilities, $R$ is the real distance between the activator and sensitizer, and $S$ is a positive integer taking the following values: $S = 6$ for dipole–dipole interactions, $S = 8$ for dipole–quadrupole interactions, and $S = 10$ for quadrupole–quadrupole interactions. It is obvious that the $P_{SA}$ depends heavily on interaction distance, thus the energy transfer is more likely to occur between neighboring $Ln^{3+}$ ions. It should be noticed that the sensitizer and activator can be either the same or different lanthanide ions.

As seen in Figure 2.2b, sometimes one excited ion can transfer part of its energy to another neighboring ion and both end up with some intermediate levels. This process is termed as "cross relaxation" (CR). Compared with ESA, ETU owns much robust UC intensity (one or two orders of magnitude

Downloaded By: 10.2.97.136 At: 04:36 30 May 2023; For: 9781315371535, chapter2, 10.1201/9781315371535

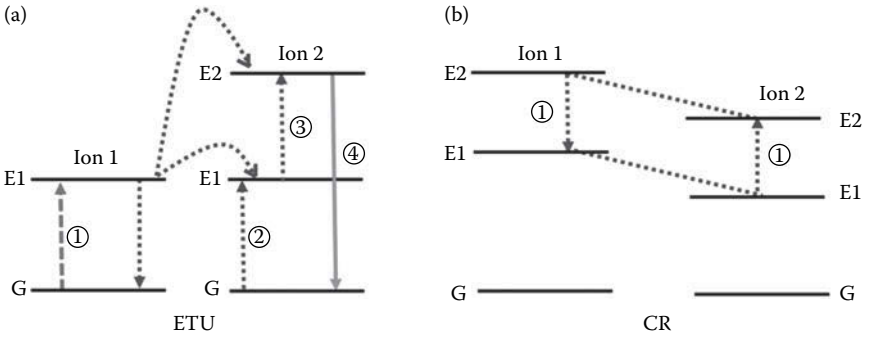


**FIGURE 2.2**
Schematic diagram of: (a) ETU and (b) CR processes.

stronger than ESA), since it has a larger absorption cross section by introducing sensitizer ions (e.g., $Yb^{3+}$ and $Nd^{3+}$) into the system. So far, ETU is the most adopted mechanism for UC applications.

The PA process was first proposed by Chivian et al. (1979). As seen in Figure 2.3, with the help of resonant CR between the excited ion and another adjacent ground state ion, the PA-induced UC process could make a feedback loop, which induces a rapid accumulative effect of the intermediate-level population, and finally leading to strong UC emission as an avalanche process. The disadvantage of PA process is that the feedback loop only works well in a very limited UC system, and furthermore, it usually requires a relatively high pump intensity (above a certain threshold) to make the feedback effective. These drawbacks have limited the PA process in practical applications.

CSU, also named as cooperative upconversion (CUC) in some literatures, is a process involving the interaction of three ions. As seen in Figure 2.4, two excited adjacent sensitizer ions cooperatively transfer the contained energy

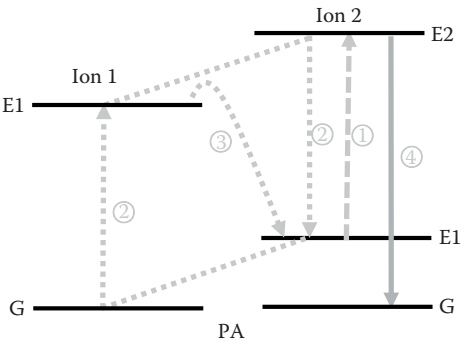


**FIGURE 2.3**
Schematic diagram of PA processes.

Downloaded By: 10.2.97.136 At: 04:36 30 May 2023; For: 9781315371535, chapter2, 10.1201/9781315371535

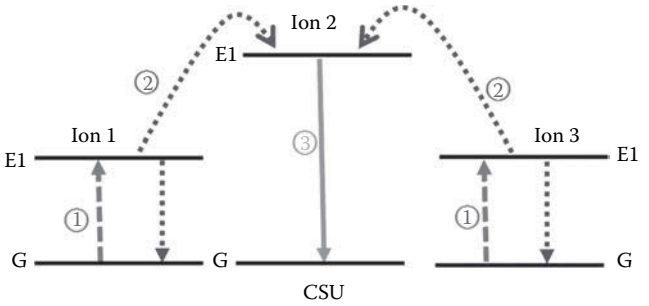


**FIGURE 2.4**
Schematic diagram of CSU processes.

to one activator ion simultaneously, and the excited activator relaxes back to its ground state by emitting an upconverted photon. Since the emitters have no intermediate energy level matchable to the sensitizer, compared with other methods, CSU reveals a much lower probability. Furthermore, although the CSU mechanism has been proposed for the $Yb^{3+}/Tb^{3+}$ or $Yb^{3+}/Eu^{3+}$ UC system (Maciel et al. 2000; Wang et al. 2008), strictly speaking, no conclusive evidence has been provided to confirm this mechanism.

### 2.1.2 EMU Mechanism

The above-mentioned traditional UC mechanisms were discovered in bulk materials, where, in order to obtain relatively strong UC emission, sensitizers and activators need to be co-doped to enhance the interaction probability between the two. Therefore, the energy transfer process (from sensitizers to activators) is popularly treated as "short-range" interaction. More specifically, activators are considered to receive energy from neighboring sensitizers directly. The treatment obviously neglects the possibility that the excitation energy of a sensitizer at a distance could in fact migrate via other sensitizers before being transferred to the activators, that is, a relatively "long-range" energy transfer interaction. Unfortunately, due to the limitations of the bulk material system, this "long-range" energy migration process has not been studied well experimentally because it is almost impossible to separate it from other UC mechanisms. Nanotechnology has made it possible to exceed the limitation in recent years. Along with the progress in synthetic technology, more and more complex UC nanostructures become possible, which enables the separation of absorption, transitions, and emission regions in different areas of a nanoparticle. In principle, after photoexcitation, the absorbed energy passes through the transition layer and reaches the activator. The energy migration processes in the transition layer could be readily studied by varying the transition layer thickness and/or the doping concentrations of the mediated ions in the layer. It

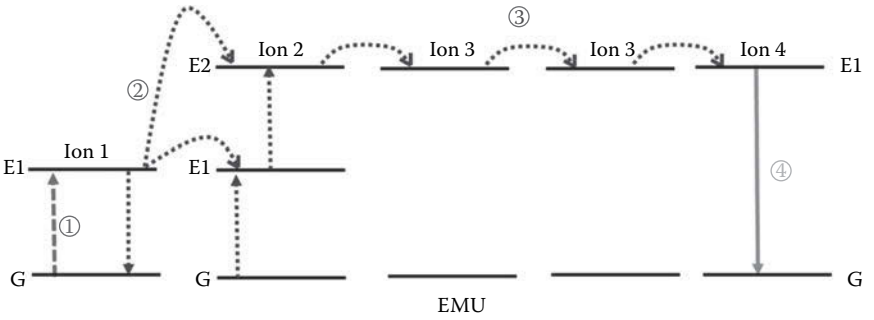


**FIGURE 2.5**
Schematic diagram of EMU processes.

has been confirmed that the excited energy can travel quite a long distance (e.g., 5 – 10 nm) without significant loss through a $Gd^{3+}$ or $Yb^{3+}$ sublattice formed transition layer (F. Wang et al. 2011; Zhong et al. 2014). The mediated ions ($Gd^{3+}$ or $Yb^{3+}$) assisted "long-range" energy migration UC phenomenon was named EMU by F. Wang et al. in 2011, as seen in Figure 2.5. The efficient "long-range" EMU process implies that the energy transfer process is actually not a local effect, and the energy could be captured by activators far away (several nanometers) from the sensitizers with the assistance of the energy migration between mediating ions. Based on this understanding, the EMU process can reasonably be assumed to play an important role in the UC process even in the traditional co-doping systems. However, this remains a subject of further study.

## 2.2 UC Dynamics

The photoluminescence (PL) dynamics is another fundamental aspect of UC emission. Compared with DC materials, the PL dynamics of UC materials has its own characteristics: (i) the measured "lifetime" of the UC emission normally will be much longer than the intrinsic lifetime of the emitting energy level and (ii) in most instances (except ESA), the UC emission usually has a rising component at the initial stage of the time evolution of UC luminescence, in relation with the population process from the long-lived sensitizers to the activators. Theoretically, the UC dynamics could be fully described by a series of differential equations for each individual $Ln^{3+}$ ion. However, these equations are too complex to be solved. One of the most commonly used simplified approaches is taking into account only the population and depopulation processes between different energy levels, and ignoring

Downloaded By: 10.2.97.136 At: 04:36 30 May 2023; For: 9781315371535, chapter2, 10.1201/9781315371535

Downloaded By: 10.2.97.136 At: 04:36 30 May 2023; For: 9781315371535, chapter2, 10.1201/9781315371535



the multi-step energy migration processes between all identical energy levels. The simplified rate equations could be described as (Chan et al. 2012)

$$\begin{aligned}\frac{dN_i}{dt} &= \sum \text{population rate} - \sum \text{depopulation rate} \\ &= \sum_j \left(N_j A_{ji}^{ED} - N_i A_{ij}^{ED}\right) + \sum_j \left(N_j A_{ji}^{MD} - N_i A_{ij}^{MD}\right) \\ &\quad + \left(N_{i+1} W_{i+1,i}^{NR} - N_i W_{i,i-1}^{NR}\right) \\ &\quad + \sum_{ij,kl} \left(N_j N_l C_{ji,lk}^{ET} - N_i N_k C_{ij,kl}^{ET}\right)\end{aligned} \tag{2.2}$$

Here, $N_i$ is the population density of each energy level, $A_{ij}^{ED}$ and $A_{ij}^{MD}$ are the Einstein coefficients for electric dipole (ED) and magnetic dipole (MD) radiative transitions from energy level $i$ to $j$. $W_{i+1,i}^{NR}$ is the nonradiative multiphonon relaxation (NMPR) rate constant from energy level $i+1$ to $i$. $C_{ij,kl}^{ET}$ is the microscopic energy transfer parameter for the transfer of energy via the sensitizer $i$ to $j$ transition and the activator $k$ to $l$ transition. The coefficients ED, MD, and $C_{ij,kl}^{ET}$ can be calculated by Judd–Ofelt theory, while the NMPR rate is treated with a modified energy gap law, and a related description of phonons is used to calculate phonon-assisted energy transfer constants. Finally, the intensity of any given UC emission is proportional to the product of the corresponding $N_i$ of each energy level and its radiative transition rates.

It should be noticed that the theoretical predictions from the rate equation (1.2) usually do not fit the experimental results well. For example, in a simplest UC system with two-level donors and three-level acceptors, it is easy to calculate from the rate equations that the UC PL decay time of the activators for $n$-photon (the value of $n$ indicates the number of excitation photons required to generate one UC photon) should be $1/n$ of the sensitizer's lifetime (Kingsley et al. 1969), which is, however, not the case in practice. Some modified dynamic models have been proposed in the past few decades. For example, the one suggested by Zusman–Burshteĭn (Artamono et al. 1972; Burshtei 1972) and Yokota–Tanimoto (Yokota and Tanimoto 1967) takes into account energy migration between sensitizers. The Zusman–Burshteĭn model fits the situation where the sensitizer–sensitizer interaction is much stronger than the sensitizer–activator one, whereas the Yokota–Tanimoto model is valid in the opposite case. On the other hand, Grant (1971) and Zubenko et al. (1997) dealt with the problem with time-dependent energy transfer rates instead of constants in the equations. Despite these efforts, the complete understanding of UC dynamics remains a challenge. In our opinion, the deviation mainly caused by (i) the uncertainty of the interaction parameters in the rate equations, (ii) the complex influence of the environment of the nanosystem, and (iii) the energy migration effect. Further investigation is needed.

Downloaded By: 10.2.97.136 At: 04:36 30 May 2023; For: 9781315371535, chapter2, 10.1201/9781315371535

## 2.3 Challenges and Recent Progress in Improving UC Luminescence in Nanosystems

The unsatisfactory UC luminescence efficiency (typically <1%) remains one of the main hurdles for application. This scenario has triggered the following questions: what are the responsible channels/steps for the loss of the excitation energy in the nanomaterials? And more interestingly, is it possible to gain even higher UC efficiency in nanomaterials than in macroscopic crystals? In order to obtain answers to these questions, a comprehensive understanding of the UC process in nanostructures is essential.

### 2.3.1 Definition of UC Efficiency and Relevant Measurement Techniques

The UC efficiency is one of the most important parameters to assess the optical performance of various UC materials. It is usually quantified by a parameter—UC luminescence quantum yield (QY), defined as the ratio of the number of UC emitted photons to the number of absorbed photons

$$\text{QY} = \frac{\text{The number of emitted photons}}{\text{The number of absorbed photons}} \tag{2.3}$$

Different from DC emission, the QY of UC luminescence is dependent on the power density of excitation light due to its nature of nonlinearity. Thus, accurate determination of the excitation power density is critical for evaluating the QY of UC luminescence.

One of the popular methods of the UC luminescence QY measurements are implemented by integrating sphere-based equipment, where the number of absorbed/emitted photons can be measured with the aid of photomultiplier tubes. It was reported that, under 150 W/cm$^2$ excitation power density, the UC QY is only 3 ± 0.3% in the $NaYF_4$: 20%Yb, 2%Er bulk material, furthermore, the value will be more than one order of magnitude lower in nano-sized materials (Boyer and van Veggel 2010).

### 2.3.2 Approaches in Enhancing UC Luminescence of Nanomaterials

In recent years, numerous efforts have been paid to enhance the luminescence efficiency or controlled spectral modulation of UC materials, especially for the nano-sized UC materials with an eye on the demand of application. Compared with bulk crystals, nano-sized materials exhibit three distinct properties which are important for their UC luminescence.

The first distinct property is the nonnegligible role of the surface properties, which is due to the relatively large surface-to-volume ratio of nanomaterials.

Downloaded By: 10.2.97.136 At: 04:36 30 May 2023; For: 9781315371535, chapter2, 10.1201/9781315371535



It is well known that the surface can form energy traps which usually quench the UC emission, but it can be beneficial to the luminescence as well. For example, enhancement and/or broadening of the absorption spectra can be realized by anchoring organic molecules or other light harvesting entities onto the surface of nanoparticles.

The second distinct property is that nanomaterials allow tailor-made internal structures. Especially due to the development of nanotechnology, more and more complex nanostructures can be constructed. This property has raised the possibility that the energy transfer paths in nanomaterials can be artificially controlled. For example, although $Nd^{3+}$ ion has a large absorption cross section in the NIR range (~800 nm), it is hardly used as sensitizers directly in bulk UC material because $Nd^{3+}$ will quench the activators' excited state population through a series of harmful CR processes. However, in a tailor-made nanostructure, for example, $NaYF_4$:Yb,Er@$NaYF_4$:Yb@$NaYF_4$:Nd core–shell–shell structure, an intense $Er^{3+}$ UC emission could be observed by restricting $Nd^{3+}$ ions in the outer layer and utilizing $Yb^{3+}$ in the middle layer to bridge energy into the inner emitting layer (Zhong et al. 2014). Another advantage of a nanostructure is that it gives the aspiration that the excitation energy might be "fully liberated" from the negative effects of lattice defects. If there is a tiny defect-free area, it can be "isolated" from the rest of the nanoparticles that might contain defects, and the absorbed energy in this area can in theory be free from nonradiative loss caused by lattice defects (Tu et al. 2015). The concentration quenching effect, which is in relation to the fact that the excitation energy migrates more easily from one ion to another under high doping concentrations which will increase the probability for the energy to be trapped by the defects inside and/or at the surface of the nanoparticles, could thus be suppressed. Therefore, a higher optimal doping concentration, that is, a higher UC efficiency, could be expected in specially designed nanostructures.

The third distinct property of nano-sized materials is that they are susceptible to the environment. Compared with bulk materials, nanomaterials are more susceptible to the environment due to their size limit, which makes external stimuli more effective in modifying UC dynamics. For example, it is possible to modify the radiative transition rate of lanthanides via the metal plasma electric field to enhance the absorption and/or UC emission intensity.

From luminescence dynamics point of view, the UC process of lanthanide ions doped systems can roughly be separated into three stages, including: excitation energy absorption, various energy transfer, and radiative release of the excitation energy, that is, emitting UC photons.

#### *2.3.2.1 Optimization of Absorption*

UC emission starts with the absorption of light. A robust UC spectrum relies not only on a high UC emission QY, but also on a large absorption cross

Downloaded By: 10.2.97.136 At: 04:36 30 May 2023; For: 9781315371535, chapter2, 10.1201/9781315371535

section. This is the starting point for developing approaches to improve UC emission. The excitation rate of state *i* can be expressed as

$$R_i \propto I_{exc}\sigma_i N_i \tag{2.4}$$

where $\sigma_i$ is the absorption cross section of state *i* at the excitation wavelength, $N_i$ is its population density, and $I_{exc}$ is the excitation density. From this relationship, it is obvious that the absorption cross section is key in determining the excitation efficiency. In recent years, optimizing the absorption of UC systems has mainly been following the $Yb^{3+}$-sensitized approach, $Yb^{3+}/Nd^{3+}$ cooperative-sensitized approach, and dye-sensitized approach.

As mentioned earlier, most of lanthanide activator ions demonstrate insufficient absorption. Furthermore, the concentration of activator ions has to be maintained at a relatively low-level (typical in a range 0.2%–5%) to avoid significant concentration quenching. Therefore, the overall UC efficiency of most activator singly doped nanocrystals is relatively low. $Er^{3+}$ is an exception in this respect, singly doped $Er^{3+}$ ion has a comparatively high UC efficiency since its optimal doping concentration can reach a relatively high level (e.g., 5%–25%) and its ladder-like energy levels are well matched with ~800, ~980, and ~1500 nm excitation. For example, under 1490 nm laser excitation, the UC QY can reach up to ~1.2 ± 0.1% under an excitation density of 150 W/cm$^2$ in a nano-sized $LiYF_4$ host (Chen et al. 2011).

Since the 1960s, Auzel et al. (1966) found that co-doped with $Yb^{3+}$ ions, the UC emission of some activators (such as $Er^{3+}$, $Tm^{3+}$, and $Ho^{3+}$) could be enhanced over 10 times. The reason is that $Yb^{3+}$ has a relatively large absorption cross section around 980 nm (several times higher than $Er^{3+}$), and its PL emission resonates well with these typical upconverting $Ln^{3+}$ ions, so the energy transfer from $Yb^{3+}$ to these $Ln^{3+}$ ions occurs effectively. Furthermore, due to the simple energy scheme of $Yb^{3+}$ ion (there is only one excited state $^2F_{5/2}$ in the energy range of interest), the harmful CR processes between $Yb^{3+}$ ions can be avoided, therefore, the "concentration quenching effect" of $Yb^{3+}$ ions is partially suppressed, so the optimal doping concentration of $Yb^{3+}$ ion in nanoparticles can reach up to 20%–40%, which strengthens its advantage. From that time on, the $Yb^{3+}$-sensitized approach was widely used to enhance the UC efficiency of $Er^{3+}$, $Tm^{3+}$, and $Ho^{3+}$ ions.

Another approach to increase the absorption of the UC system is to make better use of its spacial features. For example, a shell coating is a commonly used strategy to enhance the UC emission of a nanoparticle by separating the surface relevant quenching centers and the luminescence centers inside the core. In the majority of reported cases, the shell component is inert, that is, a shell of pure host lattice, and its sole role is to protect the luminescence centers in the core from the surface. Since 2009, a new design of the core–shell structure appeared which contains the sensitizer $Yb^{3+}$ in the shell, that is, an "active shell." The first report was on $NaGdF_4$:$Yb^{3+}$, $Er^{3+}$ nanoparticles with a shell containing 20% $Yb^{3+}$-doped $NaGdF_4$ where strong enhancement of the green and

Downloaded By: 10.2.97.136 At: 04:36 30 May 2023; For: 9781315371535, chapter2, 10.1201/9781315371535

red emission bands was realized (Vetrone et al. 2009). Additional energy transfer from excited $Yb^{3+}$ ions in the shell to the $Er^{3+}$ ions in the core was suggested to be responsible for the enhancement. However, there is also anxiety that the $Yb^{3+}$ sensitizers in the shell are harmful for UC emission since they increase the probability of the excitation energy being captured by the surface-related traps. The actual role of the active shell in UC dynamics is not clear yet.

The above-mentioned $Yb^{3+}$-sensitized UC nanoparticles, regarded as a generation of multimodal bio-probes, have been attracting wide interest in biological applications. However, the $Yb^{3+}$-sensitized UC materials have only one single narrow absorption band around 980 nm, which restricts its practical application. More recently, $Nd^{3+}$ ions are introduced as an additional NIR absorber and sensitizer in conventional $Yb^{3+}$-doped UC nanoparticles. The $Nd^{3+}$ has an even larger absorption cross section in the NIR region ($1.2 \times 10^{-19}$ cm$^2$ at 808 nm) compared to $Yb^{3+}$ ($1.2 \times 10^{-20}$ cm$^2$ at 980 nm) (Y.-F. Wang et al. 2013) and under the excitation of ~800 nm, the $Nd^{3+} - Yb^{3+}$ energy transfer efficiency is high. The disadvantage that $Nd^{3+}$ will itself quench the emission of activators due to the harmful CR process could be circumvented by a properly designed core–shell nanostructure (Y.-F. Wang et al. 2013; Xie et al. 2013; Zhong et al. 2014). The obvious superiority of the $Yb^{3+}/Nd^{3+}$ cooperative-sensitized approach is the minimization of the overheating effect in biological systems induced by water absorption (the water absorption cross section ~800 nm is much smaller than that at 980 nm).

Despite the fact that $Nd^{3+}$ and $Yb^{3+}$ ions have been excavated to enlarge the absorption ability of UC system, the f – f forbidden transition remains an essential constraint for the lanthanides. Recently, infrared organic dyes were selected as antenna ligands to enlarge the absorption spectrum for UC (Zou et al. 2012). The extinction coefficient of organic dye IR-806 at 806 nm is 390 L/g · cm, which is ~$5 \times 10^6$ times higher than that of β-$NaYF_4$:$Yb^{3+}$, $Er^{3+}$ nanoparticles at 975 nm ($7 \times 10^{-5}$ L/g · cm). The overall UC emission of the dye-sensitized nanoparticles is dramatically enhanced about 3300 times as a joint effect of the increase and overall broadening of the absorption spectrum, which was mainly ascribed to the augment of absorption. Nevertheless, most organic molecules suffer from photobleaching, which raises the concern of the photostability of the organic dye-sensitized nanomaterials.

#### *2.3.2.2 Optimization of Energy Transfer*

Energy transfer and interactions are critical for UC emission. Generally speaking, the ETU depends not only on the energy transfer between the ions, but also on the initial distribution of the excited states and the boundary conditions of the nanoparticles, for example, surface property, size, and morphology of the nanoparticles. The full description of the ETU process is therefore complex. Here, we will introduce the major factors that affect the ETU process, including the donor–acceptor combination, doping concentration, the excitation power density, and the surface effect.

Downloaded By: 10.2.97.136 At: 04:36 30 May 2023; For: 9781315371535, chapter2, 10.1201/9781315371535

Typical donor–acceptor combinations are $Yb^{3+}/Er^{3+}$, $Yb^{3+}/Ho^{3+}$, $Yb^{3+}/Tm^{3+}$, etc. It was reported that introducing some new donor–acceptor combinations can manipulate the ETU process, and consequently change the excitation and/or emission spectra of materials. For example, as mentioned earlier, the $Nd^{3+}$ – $Yb^{3+}$ cooperative-sensitized UC materials could shift the excitation of the emission to ~800 nm. On top of that, the UC emission spectrum can also be modulated by the doping elements. Single-band UC emission with high chromatic purity is known to be highly desirable for multicolor imaging, and efforts in this aspect have appeared recently in the literature based on novel donor–acceptor combinations. For example, $Er^{3+}/Tm^{3+}$ (2/2%) co-doped nanoparticles show a spectrally pure red emission (excited by 980 nm) due to the energy transfer between $Er^{3+}$ and $Tm^{3+}$ (Chan et al. 2012). However, because of the insufficient absorption of $Er^{3+}$, the UC emission is relatively weak. Alternatively, additional doping of $Mn^{2+}$ ions can bring in single-band emission in $Yb^{3+}/Er^{3+}$, $Yb^{3+}/Tm^{3+}$, and $Yb^{3+}/Ho^{3+}$ UC systems (Tian et al. 2012; J. Wang et al. 2011). Taking $Yb^{3+}/Er^{3+}$ as an example, the existence of $Mn^{2+}$ ions was considered to disturb the transition possibilities between the green and red emissions of $Er^{3+}$, with the $Er^{3+}$ – $Mn^{2+}$ energy transfer leading to depopulation of the green emitting $^2H_{11/2}$ and $^4S_{3/2}$ energy levels, and the consequent $Mn^{2+}$ – $Er^{3+}$ back energy transfer increasing the population of the red emitting energy level ($^4F_{9/2}$), resulting in an enhanced red to green emission ratio of $Er^{3+}$. In addition, doping $Ce^{3+}$ into the $Yb^{3+}/Ho^{3+}$ system could manipulate the red to green emission ratio by tuning the energy transfer process between $Ce^{3+}$ and $Ho^{3+}$ (Chen et al. 2009), and the deep-UV UC emission of $Yb^{3+}/Gd^{3+}$ combination could be enhanced by doping $Ho^{3+}$, serving as a "bridging ion" in the $Yb^{3+}$ – $Ho^{3+}$ – $Gd^{3+}$ energy transfer process (L. Wang et al. 2013).

Another potential way to improve the UC QY is to optimize the dopant concentrations within the nanoparticles. As noted before, the energy transfer process is usually considered as dipole–dipole, dipole–quadrupole, or quadrupole–quadrupole interactions and is therefore sensitive to the operating distance. The doping concentration thus significantly affects the energy transfer process. According to the reports, increasing the doping concentration of $Ln^{3+}$ ions (either sensitizer or activator) in the nanoparticles could enhance the UC emission to a certain extent. Further increase could make the cascade energy transfer process effective and the concentration quenching phenomenon significant. In practice, the optimal doping concentration of lanthanide ions is usually at a relatively low-level in the range of 0.2%–2% for activators (e.g., $Er^{3+}$, $Tm^{3+}$, or $Ho^{3+}$) with 20%–40% for sensitizer ($Yb^{3+}$). Over the years, great efforts have been made to elevate the quenching concentration of lanthanide ions in nanoparticles. Recently, there are reports that concentration quenching may be alleviated in some specially designed nanostructures. For example, in ultrasmall (7–10 nm) $NaYF_4$:x%$Yb^{3+}$, 2%$Tm^{3+}$ nanoparticles, it was demonstrated that the NIR UC emission of $Tm^{3+}$ at 808 nm increases up to 43 times along with an increase in the relative content

Downloaded By: 10.2.97.136 At: 04:36 30 May 2023; For: 9781315371535, chapter2, 10.1201/9781315371535

of $Yb^{3+}$ ions from 20% to 98% (Chen et al. 2010). However, this particularly high quenching concentration of $Yb^{3+}$ is only reported for the $Tm^{3+}$ activator co-doped case and there is no report of similar results for other activators like $Er^{3+}$ or $Ho^{3+}$. This fact might indicate that the relevant quenching mechanism needs to be further studied. On the other hand, a monotonous increase of the $Yb^{3+}$ concentration up to 98% resulting in about one order of magnitude enhancement of UC intensity in $KLu_2F_7$: x%$Yb^{3+}$, 2%$Er^{3+}$ nanoparticle has been reported (Wang et al. 2014). The specificity of the $KLu_2F_7$ crystal structure is that the doped $Yb^{3+}$ ions are separated as arrays of discrete clusters at the sublattice level and the average distance between the ionic clusters is much larger than the ionic distance within the clusters. In this crystal structure, the excitation energy absorbed by the $Yb^{3+}$ ions tends to be restricted within the discrete cluster rather than migrating a long distance toward other clusters. In this way, the concentration quenching effect can be suppressed significantly if these clusters are quenching center free.

UC emission is a typical nonlinear process. Theoretically, excitation density is directly related to the initial population of the excited states in a photoluminescent system. In the year 2000, Pollnau et al. modeled the relationship of excitation density $P$ with UC emission intensity $I$, and found that $I \propto P^n$ under low excitation power density. The value of $n$ indicates the number of NIR excitation photons required to generate one UC photon. So far, there is no evidence to suggest that the energy transfer process is dependent on the excitation density if it is relatively low, that is, <100 W/cm$^2$. Low excitation density is usually applied to the measurement of massive nanoparticles. For single nanoparticle measurements, however, high density excitation is required. It was recently, reported that under high density excitation (e.g., $2.5 \times 10^6$ W/cm$^2$) the UC emission is significantly enhanced when the concentration of activator $Tm^{3+}$ is greatly increased from 0.5% to 8% in $NaYF_4$ host (J. Zhao et al. 2013). A similar result was also observed for $Er^{3+}$ ions, co-doped with 20% $Yb^{3+}$ ions, under the low power excitation, its optimal doping concentration is ~2%, where it increases to 20% when the power density is above $3 \times 10^6$ W/cm$^2$ (Gargas et al. 2014). The proposed physical picture is based on the variety of the initial distribution of the excited state population in the nanoparticles. The higher density excitation causes more $Yb^{3+}$ ions in the excited state in the nanoparticles, and the critical step in UC emission is the excited state energy transfer from $Yb^{3+}$ to the activator ($Tm^{3+}$ or $Er^{3+}$). If the number of activators is not enough, these activators will get saturated easily in accepting excitation energy via the sensitizers. From this point of view, under excitation of high density, higher doping levels of the activator could promote the utilization of the excitation energy stored in the sensitizers, and facilitate the UC emission.

Surface characteristics of UC materials are an important issue for the efficiency of UC emission, as they expose numerous lanthanide dopants to surface deactivations (caused by surface defects, lattice strains, surface ligands, and solvents that possess high phonon energy). These processes

Downloaded By: 10.2.97.136 At: 04:36 30 May 2023; For: 9781315371535, chapter2, 10.1201/9781315371535

are strongly manifested in nanoparticles due to the high surface-to-volume ratio. Subsequently, core–shell structures were introduced to improve the UC emission and to study the surface effects of nanoparticles. By controlling the shell thickness, the direct interacting distance of surface effects to the $Ln^{3+}$ ions is confirmed to be around 1.5–5 nm (Gargas et al. 2014). And, it was reported the enhancement factor is from dozens to hundreds when the shell thickness is only 1–2 nm (Zhang et al. 2012). However, the mechanism of surface effect still needs to be clarified. It is assumed that the excited energy states situated on or near the surface can be deactivated directly by neighboring quenching centers. This understanding has loop holes for nanomaterials. For a 20 nm (diameter) sized nanoparticle, even taking the largest surface effect distance (5 nm), there is still ~12.5% area that is inert to the surface effects, which means that the maximal factor of luminescence enhancement induced by shell coating should be around eight, which is not the case. To rationalize the experimental results, an extend explanation based on EMU theory was suggested (Chen et al. 2013; Su et al. 2012): the energy contained in the excited dopants locate in the center of nanophosphors can randomly migrate and travel a long distance to the dopant on/near surface and is quenched by the surface quenching centers. However, this understanding is still half-baked, and the microscopic physical picture, especially the PL dynamics process, needs further study.

#### *2.3.2.3 Optimization of Emission*

After the absorption and energy transfer process, the UC emission arises from the depopulation of the emitting energy state, and at this stage, the competition between radiative relaxation and nonradiative relaxation rates is key to the emission intensity. As introduced earlier, for nanosystems, the relevant-doped $Ln^{3+}$ ions are more susceptible to the environment due to the limited space. External stimuli induced radiative/nonradiative rate modification is thus easier to realize in nanomaterials than in macroscopic crystals. We will restrict ourselves here to two aspects: (i) selection of host materials and (ii) plasmonic enhancement.

The phonon-induced energy loss is one of the main reasons for the low efficiency of UC emission, where the excited states' energy converts into phonons of the host via multiphonon-assisted nonradiative relaxation. A proper indicator is the cutoff phonon energy of the host lattice which is an important parameter for the selection of a good host material. Generally speaking, the higher cutoff phonon energy, the lower the UC efficiency. Compared with oxides and oxy-fluorides or oxy-chlorides hosts (lattice phonon energies >500 $cm^{-1}$), fluorides hosts (e.g., $NaYF_4$, $LiYF_4$, and $NaLuF_4$) have relative lower phonon energies (~350 $cm^{-1}$) and usually display the highest UC efficiency due to the minimization of nonradiative energy losses in the intermediate/emitting states.

As mentioned earlier, the luminescence of $Ln^{3+}$ ions is mostly due to the ED/quadrupole transitions among the energy levels of the 4f subshell. The

Downloaded By: 10.2.97.136 At: 04:36 30 May 2023; For: 9781315371535, chapter2, 10.1201/9781315371535



radiative transition is in general forbidden due to parity considerations. However, when the rare earth ions are set in an asymmetrical crystal field, the intrinsic wave functions of the 4f subshell mix with other wave functions of opposite parity, such as the wave functions of 5d, 5g, etc. The forbidden nature of the transition is thus partially broken. A highly asymmetrical crystal field is helpful in enhancing the radiative and absorption transition probabilities of rare earth ions. Some methods to change the local crystal fields in macroscopic crystals are also applied to nanosystems. For example, hexagonal $NaYF_4$:$Yb^{3+}$,$Er^{3+}$ microcrystals exhibit visible UC photoluminescence (PL), which is several times higher than their cubic counterparts. On top of that, adding certain ions (e.g., $Li^+$) into the crystal lattice is sometimes helpful to reduce the crystal symmetry and thus to enhance the UC emission intensity (C. Zhao et al. 2013). Besides tailoring the local crystal field, it was reported that the 2.7 times enhancement of UC PL could be realized in a $BaTiO_3$ (BTO) nanohost by applying a 10 V external field (Hao et al. 2011). In this work, a multilayer film material with a typical parallel plate capacitor was developed, the enhancement was argued to come from the unique crystal structure of the ferroelectric host BTO material. Tetragonal BTO with the point group 4 mm ($C_{4v}$) at room temperature is noncentrosymmetric. Upon applying an electric field along the direction of spontaneous polarization of the host, the *c*-axis of the lattice elongates and changes the structure symmetry of the BTO host. The UC emission could be enhanced in a controlled manner by simply tuning the applied electric field. The difference in the enhancement of green and red emissions was analyzed based on the Judd–Ofelt (J–O) theory. According to the authors, the green emission of $Er^{3+}$ ions comes from one of the hypersensitive transitions dominated by $\Omega_2$, which is known to be closely associated with the asymmetry of the $Ln^{3+}$ ion sites. This work points to another approach for enhancing UC emission, which could be more robust if better host materials could be explored in the future with higher breakdown voltages.

It is well known that metal nanostructures (i.e., plasmonic substrates) can enhance the emission of a fluorophore due to localized surface plasmon resonance when the distance between the metallic structure and the fluorophore is appropriate. These effects have been widely used for enhancing the downconversion fluorescence of dyes or quantum dots, and were recently introduced to UC nanomaterials. It was found that the UC PL can be enhanced by nanoparticles, nanowires, nanoshells, as well as nanoarrays of Ag and Au with enhancement 5–310-fold by optimizing pertinent experimental parameters. The enhancement could be attributed to (i) the absorption of the UC nanoparticles in relation with the excitation collection effect, (ii) the emission of the activators, and (iii) the nonradiative transition rates of $Ln^{3+}$ ions which can be changed by metal particles.

Accordingly, there are different approaches to enhance the UC emission of nanosystems using a plasmonic field. One scenario is to set the plasmonic resonance with UC emissions. Saboktakin et al. reported 5.2-fold enhancement by Au nanoparticles and 45-fold by Ag nanoparticles in UC luminescence

Downloaded By: 10.2.97.136 At: 04:36 30 May 2023; For: 9781315371535, chapter2, 10.1201/9781315371535

(Saboktakin et al. 2012). The enhancement was attributed to the increase of both the absorption and the radiative rate of the emission. Another scenario is to set the plasmonic resonance with the excitation wavelength of the UC materials (Saboktakin et al. 2013). In 2013, the plasmonic enhancement of UC PL of nanoparticles in Au nanohole arrays was reported by Saboktakin et al. In this study, Au nanohole arrays were fabricated on transparent glass substrates. By adjusting the size of the apertures, the periodicity of the array, and the thickness of the metallic layer, the plasma band of the metallic nanohole array was tuned to NIR (980 nm), which is resonate with the UC excitation. It was determined that the UC luminescence was intensified 32.6 times for the green emission at ~540 nm and 34.0 times for the red emission at ~650 nm. The authors thus came to the conclusion that the enhancements originated from the absorption improvement due to the resonance between the nanohole arrays and the excitation wavelength of the UC emission.

However, it should be noted that despite a spate of reports of plasmon-enhanced UC PL, plasmon-induced PL quenching also appears (Li et al. 2011). The quenching is attributed to the resonance energy transfer from the $Ln^{3+}$ to the metal particle or the reabsorption of the emitted light by the metal particle. Furthermore, the enhancement or quenching mechanism cannot be discriminated by time-resolved measurements, since both the interactions lead to a shorter PL decay time of $Ln^{3+}$. Therefore, more investigations are needed on the interaction between plasmonic metal nanoparticles and UC nanostructure.

## 2.4 Future Perspective

Lanthanide ions doped UC nanoparticles, emerging as a new class of luminescent material, have attracted more and more attention in recent years. However, the brightness of UC emission is still an issue for some applications, mainly caused by (i) the low efficiency of UC and (ii) the narrow and low extinction coefficient of nanoparticles. On the other hand, our comprehension of the UC mechanism is still not sufficient, especially of microscopic UC dynamics. Multidisciplinary efforts, including theoretical modeling and computation, spectroscopy, synthetic chemistry, and chemical engineering, are expected to be the solution to this formidable challenge.

## References

Artamono, M., A. Burshtei, C. M. Briskina, A. G. Skleznev, and L. D. Zusman. 1972. Time variation of $Nd^{3+}$ ion luminescence and an estimation of electron excitation migration along ions in glass. *Zh. Eksp. Teor. Fiz.* 62:863.

Downloaded By: 10.2.97.136 At: 04:36 30 May 2023; For: 9781315371535, chapter2, 10.1201/9781315371535

Auzel, F. 1966. Compteur Quantiquepar Transfert Denergie Entre Deuxionsde Terres Rares DansUn Tungstate MixteEt Dans Un Verre. *C. R. Hebd. Seances Acad. Sci. Ser. B* 262:1016.

Auzel, F. 2004. Upconversion and anti-Stokes processes with f and d ions in solids. *Chem. Rev.* 104:139–173.

Boyer, J.-C. and F. C. J. M. van Veggel. 2010. Absolute quantum yield measurements of colloidal $NaYF_4$: $Er^{3+}$, $Yb^{3+}$ upconverting nanoparticles. *Nanoscale* 2:1417–1419.

Burshtei, A. 1972. Jump mechanism of energy-transfer. *Zh. Eksp. Teor. Fiz.* 62:1695.

Chan, E. M., G. Han, J. D. Goldberg et al. 2012. Combinatorial discovery of lanthanide-doped nanocrystals with spectrally pure upconverted emission. *Nano Lett.* 12:3839–3845.

Chen, G., H. Liu, G. Somesfalean, H. Liang, and Z. Zhang. 2009. Upconversion emission tuning from green to red in $Yb^{3+}$/$Ho^{3+}$-codoped $NaYF_4$ nanocrystals by tridoping with $Ce^{3+}$ ions. *Nanotechnology* 20:385704.

Chen, G., T. Y. Ohulchanskyy, A. Kachynski, H. Agren, and P. N. Prasad. 2011. Intense visible and near-infrared upconversion photoluminescence in colloidal $LiYF_4$: $Er^{3+}$ nanocrystals under excitation at 1490 nm. *ACS Nano* 5:4981–4986.

Chen, G., T. Y. Ohulchanskyy, R. Kumar, H. Agren, and P. N. Prasad. 2010. Ultrasmall monodisperse $NaYF_4$:$Yb^{3+}$/$Tm^{3+}$ nanocrystals with enhanced near-infrared to near-infrared upconversion photoluminescence. *ACS Nano* 4:3163–3168.

Chen, G., C. Yang, and P. N. Prasad. 2013. Nanophotonics and nanochemistry: Controlling the excitation dynamics for frequency up- and down-conversion in lanthanide-doped nanoparticles. *Acc. Chem. Res.* 46:1474–1486.

Chivian, J. S., W. E. Case, and D. D. Eden. 1979. The photon avalanche—A new phenomenon in $Pr^{3+}$-based infrared quantum counters. *Appl. Phys. Lett.* 35:124–125.

Gargas, D. J., E. M. Chan, A. D. Ostrowski et al. 2014. Engineering bright sub-10-nm upconverting nanocrystals for single-molecule imaging. *Nat. Nanotechnol.* 9:300–305.

Grant, W. J. C. 1971. Role of rate equations in theory of luminescent energy transfer. *Phys. Rev. B Solid State* 4:648.

Hao, J., Y. Zhang, and X. Wei. 2011. Electric-induced enhancement and modulation of upconversion photoluminescence in epitaxial $BaTiO_3$:Yb/Er thin films. *Angew. Chem. Int. Ed.* 50:6876–6880.

Kingsley, J. D., G. E. Fenner, and S. V. Galginai. 1969. Kinetic and efficiency of infrared-to-visible conversion in $LaF_3$–Yb, Er. *Appl. Phys. Lett.* 15:115.

Li, Z., L. Wang, Z. Wang, X. Liu, and Y. Xiong. 2011. Modification of $NaYF_4$:Yb,Er@ $SiO_2$ nanoparticles with gold nanocrystals for tunable green-to-red upconversion emissions. *J. Phys. Chem. C* 115:3291–3296.

Maciel, G. S., A. Biswas, R. Kapoor, and P. N. Prasad. 2000. Blue cooperative upconversion in $Yb^{3+}$-doped multicomponent sol–gel-processed silica glass for three-dimensional display. *Appl. Phys. Lett.* 76:1978–1980.

Saboktakin, M., X. Ye, U. K. Chettiar et al. 2013. Plasmonic enhancement of nanophosphor upconversion luminescence in Au nanohole arrays. *ACS Nano* 7:7186–7192.

Saboktakin, M., X. Ye, S. J. Oh et al. 2012. Metal-enhanced upconversion luminescence tunable through metal nanoparticle–nanophosphor separation. *ACS Nano* 6:8758–8766.

Su, Q., S. Han, X. Xie et al. 2012. The effect of surface coating on energy migration-mediated upconversion. *J. Am. Chem. Soc.* 134:20849–20857.

Downloaded By: 10.2.97.136 At: 04:36 30 May 2023; For: 9781315371535, chapter2, 10.1201/9781315371535

Tian, G., Z. Gu, L. Zhou et al. 2012. $Mn^{2+}$ dopant-controlled synthesis of $NaYF_4$:Yb/Er upconversion nanoparticles for *in vivo* imaging and drug delivery. *Adv. Mater.* 24:1226–1231.

Tu, L. P., X. M. Liu, F. Wu, and H. Zhang. 2015. Excitation energy migration dynamics in upconversion nanomaterials. *Chem. Soc. Rev.* 44:1331–1345.

Vetrone, F., R. Naccache, V. Mahalingam, C. G. Morgan, and J. A. Capobianco. 2009. The active-core/active-shell approach: A strategy to enhance the upconversion luminescence in lanthanide-doped nanoparticles. *Adv. Funct. Mater.* 19:2924–2929.

Wang, F., R. Deng, J. Wang et al. 2011. Tuning upconversion through energy migration in core–shell nanoparticles. *Nat. Mater.* 10:968–973.

Wang, H., C.-K. Duan, and P. A. Tanner. 2008. Visible upconversion luminescence from $Y_2O_3$:$Eu^{3+}$,$Yb^{3+}$. *J. Phys. Chem. C* 112:16651–16654.

Wang, J., R. Deng, M. A. MacDonald et al. 2014. Enhancing multiphoton upconversion through energy clustering at sublattice level. *Nat. Mater.* 13:157–162.

Wang, J., F. Wang, C. Wang, Z. Liu, and X. Liu. 2011. Single-band upconversion emission in lanthanide-doped $KMnF_3$ Nanocrystals. *Angew. Chem. Int. Ed.* 50:10369–10372.

Wang, L., M. Lan, Z. Liu et al. 2013. Enhanced deep-ultraviolet upconversion emission of $Gd^{3+}$ sensitized by $Yb^{3+}$ and $Ho^{3+}$ in beta-$NaLuF_4$ microcrystals under 980 nm excitation. *J. Mater. Chem. C* 1:2485–2490.

Wang, Y.-F., G.-Y. Liu, L.-D. Sun et al. 2013. $Nd^{3+}$-sensitized upconversion nanophosphors: Efficient *in vivo* bioimaging probes with minimized heating effect. *ACS Nano* 7:7200–7206.

Xie, X., N. Gao, R. Deng et al. 2013. Mechanistic investigation of photon upconversion in $Nd^{3+}$-sensitized core–shell nanoparticles. *J. Am. Chem. Society* 135:12608–12611.

Yokota, M. and O. Tanimoto. 1967. Effects of diffusion on energy transfer by resonance. *Journal of the Physical Society of Japan* 22:779.

Zhang, F., R. Che, X. Li et al. 2012. Direct imaging the upconversion nanocrystal core/shell structure at the subnanometer level: Shell thickness dependence in upconverting optical properties. *Nano Lett.* 12:2852–2858.

Zhao, C., X. Kong, X. Liu et al. 2013. $Li^+$ ion doping: An approach for improving the crystallinity and upconversion emissions of $NaYF_4$:$Yb^{3+}$, $Tm^{3+}$ nanoparticles. *Nanoscale* 5:8084–8089.

Zhao, J., D. Jin, E. P. Schartner et al. 2013. Single-nanocrystal sensitivity achieved by enhanced upconversion luminescence. *Nat. Nanotechnol.* 8:729–734.

Zhong, Y., G. Tian, Z. Gu et al. 2014. Elimination of photon quenching by a transition layer to fabricate a quenching-shield sandwich structure for 800 nm excited upconversion luminescence of $Nd^{3+}$ sensitized nanoparticles. *Adv. Mater.* 26:2831–2837.

Zou, W., C. Visser, J. A. Maduro, M. S. Pshenichnikov, and J. C. Hummelen. 2012. Broadband dye-sensitized upconversion of near-infrared light. *Nat. Photonics* 6:560–564.

Zubenko, D. A., M. A. Noginov, V. A. Smirnov, and I. A. Shcherbakov. 1997. Different mechanisms of nonlinear quenching of luminescence. *Phys. Rev. B* 55:8881–8886.